

Transverse Spin Seebeck Effect versus Anomalous and Planar Nernst Effects in Permalloy Thin Films

M. Schmid,¹ S. Srichandan,¹ D. Meier,² T. Kuschel,² J.-M. Schmalhorst,² M. Vogel,¹ G. Reiss,² C. Strunk,¹ and C. H. Back¹

¹*Institute of Experimental and Applied Physics, University of Regensburg, D-93040 Regensburg, Germany*

²*Department of Physics, Thin Films and Physics of Nanostructures, Bielefeld University, D-33501 Bielefeld, Germany*

(Received 28 March 2013; revised manuscript received 18 June 2013; published 28 October 2013)

Transverse magnetothermoelectric effects are studied in Permalloy thin films grown on MgO and GaAs substrates and compared to those grown on suspended SiN_x membranes. The transverse voltage along platinum strips patterned on top of the Permalloy films is measured versus the external magnetic field as a function of the angle and temperature gradients. After the identification of the contribution of the planar and anomalous Nernst effects, we find an upper limit for the transverse spin Seebeck effect, which is several orders of magnitude smaller than previously reported.

DOI: [10.1103/PhysRevLett.111.187201](https://doi.org/10.1103/PhysRevLett.111.187201)

PACS numbers: 85.75.-d, 72.15.Jf, 85.80.-b

The field of spin caloritronics [1] connects spin and thermoelectric transport phenomena including spin dependent thermopower [2], thermal spin transfer torque [3], spin [4] and anomalous Nernst effects [5,6], and spin Seebeck tunneling [7]. A novel effect called the spin Seebeck effect (SSE) has recently attracted attention since it may be appealing to control pure spin currents using thermal gradients. In general, the SSE has been observed in two distinct sample configurations, namely, transverse (TSSE) and longitudinal (LSSE). In the case of TSSE a spin current is generated perpendicular to a thermal gradient $\vec{\nabla}T$. In the standard TSSE setup $\vec{\nabla}T$ is applied in the plane of an in-plane magnetized ferromagnetic layer (FM). In case of LSSE a spin current is generated parallel to $\vec{\nabla}T$, which is typically applied out-of-plane to a FM/NM bilayer. In both cases transverse voltages arising from the inverse spin Hall effect (ISHE) are measured along normal metal (NM) strips or layers, with high spin-orbit interaction [8,9]. For ISHE detection of a spin imbalance in, e.g., Pt, the transverse electromotive force is given by $E_{\text{ISHE}} = D_{\text{ISHE}} J_s \times \sigma$, where D_{ISHE} is the ISHE efficiency, J_s the spin current entering the NM, and σ is the spin polarization vector of the FM. TSSE has been observed in metallic [10–12], semiconducting [13], and insulating [14] ferromagnetic films. SSEs have been observed at low as well as at room temperature [15,16].

The first observation of TSSE was on Permalloy (Py) films on sapphire substrates [10]. The authors suggested that the origin of the effect was the difference of the chemical potentials of the spin-up and spin-down electrons at the Fermi level. This explanation had to be discarded because the signal was observable at distances much larger than the spin diffusion length of the FM. Next, the effect was detected in the diluted magnetic semiconductor GaMnAs [13]. Small scratches interrupting the FM film did not change the signal, which indicates an important

role played by the phonons in the substrate. SSE was observed in the insulating ferrimagnets LaY₂Fe₅O₁₂ (LSSE [14]) and Y₂Fe₅O₁₂ (TSSE [17]) where J_s can only be transported by magnons. These observations gave rise to a recent explanation of the SSE in terms of phonon-magnon and phonon-electron drag effects mediated through the substrate [18].

Notwithstanding the rapid advancement in this field, key issues of the SSE are not well understood. For instance, there is little agreement on the value of the spin-Hall angle of Pt [9,19] leading to an uncertainty in the evaluation of the spin Seebeck coefficient S_S . Additionally, in metallic FMs such as Py, other magnetothermoelectric effects may contribute to the measured transverse voltage. Huang *et al.* [6] performed measurements on Py films deposited on bulk silicon substrates. Their results suggest that the transverse voltage generated by the out-of-plane temperature gradient due to the anomalous Nernst effect (ANE) in the bulk substrate overpowers the TSSE on the ferromagnetic thin film by a few orders of magnitude. In an attempt to resolve this question and understand the role of the substrate, Avery *et al.* conducted experiments on 500 nm thick suspended SiN_x membranes in the transverse geometry [20]. In their study they observe the planar Nernst effect [21], i.e., the off-diagonal element S_{xy} of the anisotropic magnetothermopower (AMTEP) tensor \mathbf{S} , which is the thermal equivalent to the tensor of the anisotropic magnetoresistance. No detectable contribution of the TSSE was found in that study. Hence, a systematic study of Py films on bulk substrates as well as on suspended thin membranes is required to elucidate the role of the substrate and to discriminate the TSSE from other magnetothermoelectric effects.

In this study we report on transverse thermoelectric effects in Py thin films on bulk MgO and GaAs substrates as well as on 100 nm thick SiN_x membranes. The various effects contributing to the transverse voltage can be

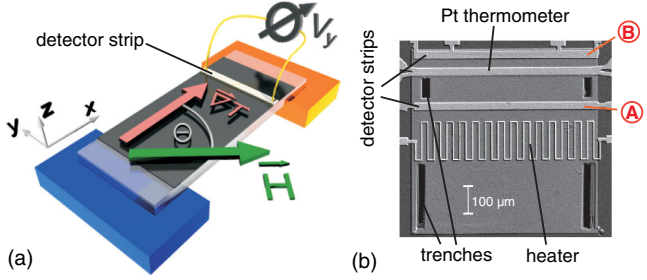


FIG. 1 (color online). (a) Setup 1: A Py film of $4 \times 8 \text{ mm}^2$ size on a $4 \times 10 \text{ mm}^2$ MgO substrate is subjected to a temperature gradient $\vec{\nabla}_x T$ along the x axis between two Peltier elements with 7 mm spacing. The transverse voltage V_y is probed with bond wires on both ends of the Pt detector strip. The magnetic field \vec{H} is applied in the film plane at an angle of Θ to the x axis. (b) Setup 2: A similar Py film patterned on a $500 \times 500 \mu\text{m}^2$ SiN_x membrane. Besides an electrically isolated heater and thermometers two Pt detector strips labeled A and B are used.

distinguished by virtue of the angular dependence of the transverse voltage and can be understood in terms of the AMTEP and the ANE, while possible contributions from the TSSE are significantly smaller than previously reported for samples on bulk substrates.

Two types of setups were investigated for the experiments. Setup 1: Py films of 20 nm thickness were sputter deposited onto GaAs or electron-beam evaporated onto MgO substrates at a base pressure of 10^{-8} mbar. Without breaking the vacuum, a single $100 \mu\text{m}$ wide and 10 nm thick Pt strip was sputtered *in situ* through shadow masks onto the Py films; see Fig. 1(a). In order to establish a controlled and reproducible temperature gradient, we mount the bulk substrate devices onto two temperature stabilized Peltier elements that are attached to a common copper block as a heat sink allowing control of the temperature gradients for various base temperatures. The whole system is placed in a vacuum chamber with a base

pressure of 2×10^{-6} mbar in order to suppress any influence of convection. In control measurements, the local temperatures on the film were determined independently using thermocouples. A pair of rotatable Helmholtz coils enables magnetic field sweeps in the sample plane at different angles Θ between the temperature gradient $\vec{\nabla}_x T$ and the magnetic field \vec{H} . To minimize heat leaks by the electric contacts thin ($50 \mu\text{m}$) and 20 mm long Au bond wires were glued to both ends of the single Pt detector strip using silver epoxy spots with a diameter below $100 \mu\text{m}$. The strip is located asymmetrically near one edge of the Py film.

Setup 2: Bilayers with 20 nm of Py and 10 nm of Pt have been sputter deposited *in situ* at a base pressure of 10^{-8} mbar onto $500 \times 500 \mu\text{m}^2$ large and 100 nm thick freely suspended SiN_x membranes. Leaving two $20 \mu\text{m}$ wide Pt strips [A, B in Fig. 1(b)] on the Py film, the rest of the Pt layer was removed by Ar etching. Contacts to these Pt detector strips have been made by a subsequent *e*-beam lithography step. A meandering 40 nm thick Au heater wire is located at the center of the membrane and close to one of the Pt strips. The heater and thermometers are electrically isolated from the Py film using 30 nm Al_2O_3 . To provide a homogeneous temperature gradient between the heater and the heat sink, trenches have been cut into the SiN_x membrane (black regions) near the edges using a focused ion beam [see Fig. 1(b)]. Setup 2 was investigated in a different vacuum system at a base pressure of 10^{-6} mbar.

Since for the observation of SSE the interfaces are important [14], we verified the high quality of the FM/NM interfaces by performing spin pumping experiments on identical Pt/Py bilayers and find a spin mixing conductance $g^{\uparrow\downarrow} \approx 2 \times 10^{15} \text{ cm}^{-2}$.

Figures 2(a) and 2(b) display the transverse voltage V_y measured while sweeping the magnetic field at different angles Θ in setups 1 and 2, respectively. We first focus on

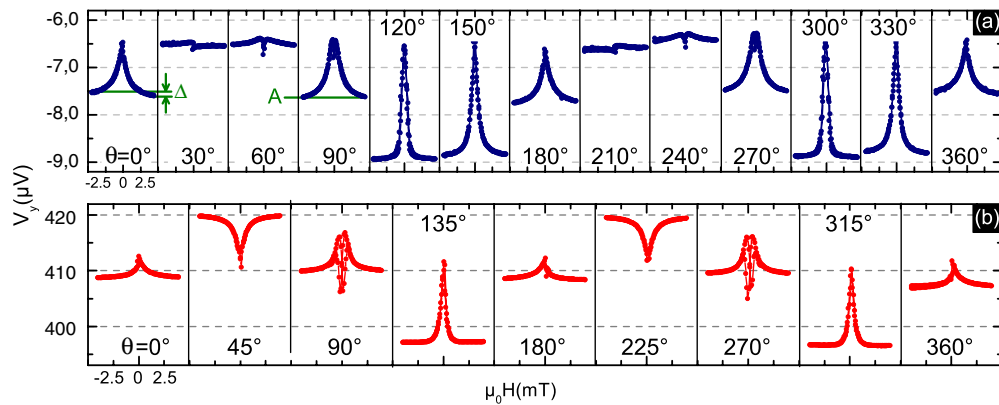


FIG. 2 (color online). Transverse voltage V_y versus the magnetic field and angle Θ . (a) Setup 1: Py on the MgO substrate; $-4.5 \leq \mu_0 H \leq 4.5 \text{ mT}$, $\vec{\nabla}_x T \approx 3.6 \text{ K/mm}$. The noise level in each sweep is 10 nV. (b) Setup 2: Py on the SiN_x membrane; $-4 \leq \mu_0 H \leq 4 \text{ mT}$, $\vec{\nabla}_x T \approx 240 \text{ K/mm}$ is applied over a distance of $200 \mu\text{m}$. Data are obtained at strip A in Fig. 1(b). The noise level in each sweep is 50 nV.

setup 1 [see Fig. 1(a)]. The temperatures of the Peltier elements were set to 343 K (hot) and 293 K (cold). Taking into account the thermal resistance of the junction interfaces, this results in a temperature difference of (25 ± 5) K ($\vec{\nabla}_x T \cong 3.6$ K/mm) across the Py film. Figure 2 shows three main contributions to $V_y(H)$: sharp maxima or minima located around $H = 0$, an oscillation of the base line, i.e., the average $A(\Theta) = [V_y^- + V_y^+]/2$ of the saturation values V_y^\pm evaluated for $H \gtrsim 4$ mT, and a small asymmetry $\Delta(\Theta) = V_y^- - V_y^+$ of V_y^\pm with respect to the orientation of \vec{H} .

The prominent peak or dip structure near $H = 0$ and the oscillation of the base line $A(\Theta)$ arise naturally from the off-diagonal element $S_{xy}(\Theta)$ of the tensor \mathbf{S} of the AMTEP that locally connects the transverse electric field E_y with $\vec{\nabla}_x T$. S_{xy} has to vanish if \vec{M} is aligned with one of the two principal axes of \mathbf{S} , i.e., when the angle ϕ between \vec{M} and $\vec{\nabla}_x T$ is equal to $0^\circ, 90^\circ, 180^\circ$, or 270° during the magnetization reversal process. Maximal (minimal) values of V_y are observed, when $\phi = 45^\circ, 225^\circ$ ($135^\circ, 315^\circ$). The variation of V_y with H at a fixed angle results from the rotation of ϕ during the magnetization reversal process. If Θ coincides with the orientation Θ_e of the easy axis of the film we have $\phi, \Theta = \text{const}$, and $V_y(H)$ remains essentially constant. Hence, we can infer $\Theta_e \approx 35^\circ$ from Fig. 2(a). The small uniaxial magnetic anisotropy arises from a residual magnetic field during deposition [22,23].

As shown in Fig. 3(a) the variation of the base line follows $A(\Theta) = 2A_0 \sin(\Theta) \cos(\Theta) + c$ [21] with an amplitude $A_0 \approx 1.2 \mu\text{V}$ and a contribution c that is independent of Θ . In contrast, the asymmetry $\Delta = \Delta_0 \cos(\Theta)$ of the saturation values V_y^\pm plotted in Fig. 3(b) follows a simpler cosine dependence with an amplitude $\Delta_0 \approx 50$ nV. The angle dependence of Δ is consistent with both the TSSE and the ANE.

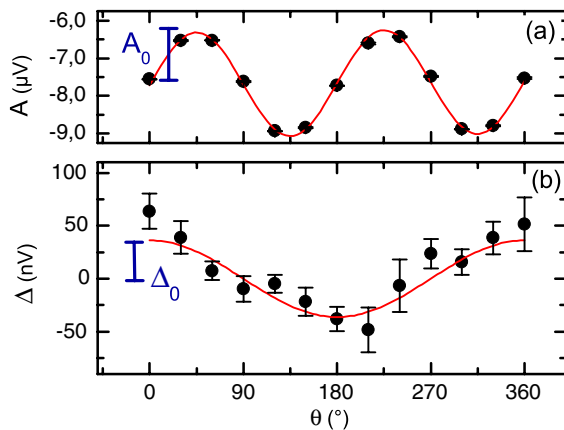


FIG. 3 (color online). Average A (a) and difference Δ (b) of the saturation values from Fig. 2(a) as a function of angle Θ . The red lines show the $2A_0 \sin(\Theta) \cos(\Theta) + c$ fit for (a) and the $\Delta_0 \cos(\Theta)$ fit for (b).

Further measurements have been performed at different base temperatures with three fixed temperature differences $(\Delta T)_x = 0$ and ± 25 K. In Fig. 4 we plot the resulting values of Δ_0 and A_0 versus the local temperature at the Pt strip T_{strip} . The inset shows values of A_0 with an average around $0.8 \mu\text{V}$ for $(\Delta T)_x = 25$ K with a changing sign for opposite temperature gradient direction. Within the scatter the value of A_0 is essentially independent of base temperature. As expected for a thermovoltage, A_0 vanishes in the absence of an in-plane temperature gradient [$(\Delta T)_x = 0$ K].

The asymmetry amplitude Δ_0 in Fig. 4 increases as a function of T_{strip} . In contrast to A_0 , Δ_0 remains finite even for $(\Delta T)_x = 0$ K, and is comparable in magnitude to the data for $(\Delta T)_x = \pm 25$ K. This proves that the monotonic increase of Δ_0 with increasing T_{strip} cannot be attributed to the TSSE, but has to be related to yet another magneto-thermoelectric effect with the same $\cos(\Theta)$ symmetry.

To study the influence of the substrate on the presence of transverse voltages, additional measurements have been performed on GaAs with the same Py film dimensions as described above. The AMTEP exhibits qualitatively similar temperature dependencies as on the MgO substrate and also Δ_0 shows a similar behavior as on MgO (see the Supplemental Material [24]).

As the origin of the finite $\Delta_0[(\Delta T)_x = 0$ K], we suggest an out-of-plane temperature gradient $\vec{\nabla}_z T$ producing a transverse voltage V_y due to the ANE. In order to estimate the values of $\vec{\nabla}_z T$ that may generate the measured $\cos\Theta$ dependence of the transversal voltage, a finite element simulation has been performed (see Fig. 4, the solid line and right scale bar). $\vec{\nabla}_z T_z$ of a few nK/nm turns out to be sufficient to generate voltages of the measured order of magnitude. The model includes surface to surface radiation

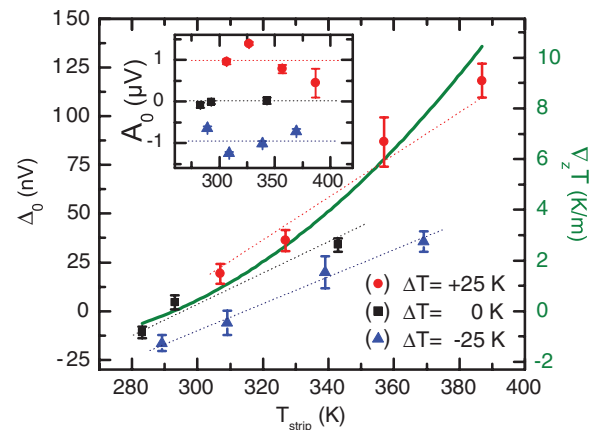


FIG. 4 (color). Δ_0 versus the temperature at the Pt strip position for different $\vec{\nabla}_x T$. The inset shows the related average values A_0 . The measurements are taken on a single MgO substrate. The green line indicates the results of the finite element simulation. The dotted lines are a guide to the eye.

of two black bodies, i.e., the sample surface and a heat sink at room temperature at a few centimeters distance simulating the geometry of setups. Taking the sample dimensions into account, $\vec{\nabla}_z T$ transforms to V_y using $\vec{\nabla} V_{\text{ANE}} = -\alpha \hat{m} \times \vec{\nabla} T_z$ with the magnetic unity vector \hat{m} and the anomalous Nernst coefficient $\alpha = 2.6 \mu\text{V}/\text{K}$ [6]. The calculated values (Fig. 4, the solid line and left scale bar) are in good agreement with the experimental data concerning magnitude and temperature dependence.

In addition to the ANE contribution, the traces for $(\Delta T)_x = \pm 25 \text{ K}$ are shifted up (down) with respect to the $(\Delta T)_x = 0 \text{ K}$ data (Fig. 4). This asymmetry of the order of 50 nV may be related to the TSSE which is expected to change sign for opposite $\vec{\nabla}_x T$.

To verify that this contribution indeed arises from the TSSE, we exchanged the Pt strip with a Cu strip, as Cu should reduce the ISHE and thus the TSSE contribution drastically. The Δ_0 signal again exhibits finite values for $(\Delta T)_x = 0 \text{ K}$ and the data points for opposite $(\Delta T)_x$ are still shifted by a few tens of nV probably due to the asymmetric positioning of the Pt strip (see the Supplemental Material [24]). Taking this into account we measure no TSSE contribution within our detection limit of $\Delta_0 = 20 \text{ nV}$. Taking this as an upper limit of TSSE, we estimate the spin Seebeck coefficient S_S in the same way as Uchida *et al.* [10]: $S_S = 2\Delta_0 d_{\text{Pt}} / [\Theta_H \eta l_{\text{Pt}} (\Delta T)_x]$ with Pt thickness d_{Pt} , the length of the Pt strip l_{Pt} , the spin-Hall angle $\Theta_H = 0.0037$, and the spin injection efficiency $\eta = 0.2$. We find an upper limit of $S_S = -5.4 \text{ pV}/\text{K}$ for our data, which is about 2 orders of magnitude smaller than what is reported for comparable temperature differences and sample dimensions [10].

To verify whether the observed effects depend on the phonons of a massive substrate, we deposited the Py film on a suspended 100 nm thin SiN_x membrane [see Fig. 1(b)]. For the suspended films all measurements have been performed at a base temperature of $(280 \pm 0.5) \text{ K}$. Figure 2(b) shows the angular dependence of the voltage traces obtained from Pt strip A (close to the heater). Measurements with Pt strip B (cold side) resulted in identical curves. The data obtained from the suspended film exhibit similar sinusoidal dependence as the Py film on bulk substrate [see Fig. 2(a)] but with a magnetic easy axis $\Theta_e \approx 190^\circ$. The data were treated as before: V_y again follows $A = 2A_0 \sin(\Theta) \cos(\Theta) + c$ with an amplitude A_0 of about $10 \mu\text{V}$ (see the Supplemental Material [24]). The higher offset values result from different wiring conditions in setup 2. In contrast to the samples on a bulk substrate, Δ shows no $\cos(\Theta)$ dependence. Within the estimated error, Δ_0 does not exceed $\approx 250 \text{ nV}$ (see the Supplemental Material [24]). Using the value of $S_S = -2 \text{ nV}/\text{K}$ given by Uchida *et al.* [10], one would expect a TSSE contribution to Δ_0 of around $2 \mu\text{V}$. This is clearly not observed. On the other hand, starting with $\Delta_0 = 250 \text{ nV}$ as the experimental input, the resulting upper limit of S_S on the

membrane is $-0.3 \text{ nV}/\text{K}$ which is 1 order of magnitude smaller than published [10]. In addition, we measured V_y on the suspended Py films without the Pt strip and found very similar results (see the Supplemental Material [24]). This shows that a possible voltage resulting from TSSE is a minor contribution in our experiment.

The absence of TSSE in the measurements of Avery *et al.* [20] may be related to the much lower phonon density of states in the thin suspended SiN_x membrane as it was proposed that the TSSE is a phonon mediated effect [18]. In this study we confirm the absence of TSSE in suspended Py films on 5 times thinner SiN_x membranes. In addition, the TSSE observed in our Py films on bulk MgO and GaAs substrates was at most a few tens of nV despite the fact that we ensured a high transparency of the Py/Pt interface. Such small values for Py films both on suspended SiN_x membranes and on bulk substrates suggest that the phonons in the bulk substrate are of minor relevance for the reported observations of the TSSE in Py films [10–12], and that our observations can be attributed to a large extent to the anisotropic spin scattering in the Py.

In conclusion, we have shown that for Py/Pt films on both bulk substrates as well as membranes, the dominant contribution to the transverse signal obtained in a TSSE geometry results from the anisotropic magnetothermopower. In addition, an appreciable contribution from the ANE originating from an out-of-plane temperature gradient is present. Independent of the presence or absence of phonons a contribution of the TSSE can be neglected within our detection limits.

The authors gratefully acknowledge financial support by the DFG within SpinCaT (SPP 1538) and the BMBF.

-
- [1] G. E. W. Bauer, A. H. MacDonald, and S. Maekawa, *Solid State Commun.* **150**, 459 (2010).
 - [2] A. Slachter, F. L. Bakker, J.-P. Adam, B. J. Van Wees, *Nat. Phys.* **6**, 879 (2010).
 - [3] M. Hatami, G. E. W. Bauer, Q. Zhang, and P. J. Kelly, *Phys. Rev. Lett.* **99**, 066603 (2007).
 - [4] X. Liu and X. C. Xie, *Solid State Commun.* **150**, 471 (2010).
 - [5] Y. Pu, E. Johnston-Halperin, D. D. Awschalom, and J. Shi, *Phys. Rev. Lett.* **97**, 036601 (2006).
 - [6] S. Y. Huang, W. G. Wang, S. F. Lee, J. Kwo, and C. L. Chien, *Phys. Rev. Lett.* **107**, 216604 (2011).
 - [7] J.-C. Le Breton, S. Sharma, H. Saito, S. Yuasa, and R. Jansen, *Nature (London)* **475**, 82 (2011).
 - [8] R. H. Silsbee, A. Janossy, and P. Monod, *Phys. Rev. B* **19**, 4382 (1979).
 - [9] T. Kimura, Y. Otani, T. Sato, S. Takahashi, and S. Maekawa, *Phys. Rev. Lett.* **98**, 156601 (2007).
 - [10] K. Uchida, S. Takahashi, K. Harii, J. Ieda, W. Koshibae, A. Ando, S. Maekawa, and E. Saitoh, *Nature (London)* **455**, 778 (2008).
 - [11] K. Uchida, T. Ota, K. Harii, K. Ando, H. Nakayama, and E. Saitoh, *J. Appl. Phys.* **107**, 09A951 (2010).

- [12] S. Bosu, Y. Sakuraba, K. Uchida, K. Saito, T. Ota, E. Saitoh, and K. Takanashi, *Phys. Rev. B* **83**, 224401 (2011).
- [13] C. M. Jaworski, J. Yang, S. Mack, D. D. Awschalom, J. P. Heremans, and R. C. Myers, *Nat. Mater.* **9**, 898 (2010).
- [14] K. Uchida, J. Xiao, H. Adachi, J. Ohe, S. Takahashi, J. Ieda, T. Ota, Y. Kajiwara, H. Umezawa, H. Kawai, G. E. W. Bauer, S. Maekawa, and E. Saitoh, *Nat. Mater.* **9**, 894 (2010).
- [15] D. Meier, T. Kuschel, L. Shen, A. Gupta, T. Kikkawa, K. Uchida, E. Saitoh, J.-M. Schmalhorst, and G. Reiss, *Phys. Rev. B* **87**, 054421 (2013)
- [16] C. M. Jaworski, J. Yang, S. Mack, D. D. Awschalom, R. C. Myers, and J. P. Heremans, *Phys. Rev. Lett.* **106**, 186601 (2011)
- [17] K. Uchida, H. Adachi, T. Ota, H. Nakayama, S. Maekawa, and E. Saitoh, *Appl. Phys. Lett.* **97**, 172505 (2010).
- [18] H. Adachi, K. Uchida, E. Saitoh, J. Ohe, S. Takahashi, and S. Maekawa, *Appl. Phys. Lett.* **97**, 252506 (2010).
- [19] K. Ando, S. Takahashi, K. Harii, K. Sasage, J. Ieda, S. Maekawa, and E. Saitoh, *Phys. Rev. Lett.* **101**, 036601 (2008).
- [20] A. D. Avery, M. R. Pufall, and B. L. Zink, *Phys. Rev. Lett.* **109**, 196602 (2012).
- [21] V. D. Ky, *Phys. Status Solidi* **22**, 729 (1967);
- [22] S. Chikazumi, *J. Phys. Soc. Jpn.* **11**, 551 (1956).
- [23] J. F. Dillinger and R. M. Bozorth, *Physics* **6**, 279 (1935).
- [24] See Supplemental Material at <http://link.aps.org/supplemental/10.1103/PhysRevLett.111.187201> for measurements of the exchange of the strip material from Pt to Cu as well as for data obtained on the GaAs substrate and the SiN_x membrane. Further information about negligible contributions of an out of plane magnetization component and of a temperature gradient along the detector strip is provided.